Supporting Information

Supramolecular Hybrids of MoS_2 and Graphene Nanosheets with Organic Chromophores for Optoelectronic Applications

Manjodh Kaur[†], Navin Kumar Singh[‡], Aritra Sarkar[‡], Subi J. George*[‡] and C. N. R. Rao*[†‡]

[†]Sheikh Saqr Laboratory, International Centre for Materials Science, School of Advanced Materials, Jawaharlal Nehru Centre for Advanced Scientific Research, Jakkur, P. O., Bangalore 560064, India

[‡]School of Advanced Materials and New Chemistry Unit, Jawaharlal Nehru Centre for Advanced Scientific Research , Jakkur, P. O., Bangalore 560064, India

*E-mail: george@jncasr.ac.in; cnrrao@jncasr.ac.in

Supporting figures and synthetic procedures:

Synthetic procedures:

Scheme S1. Synthetic route for synthesising a) **NMI-im** and b) **Nap-im**.

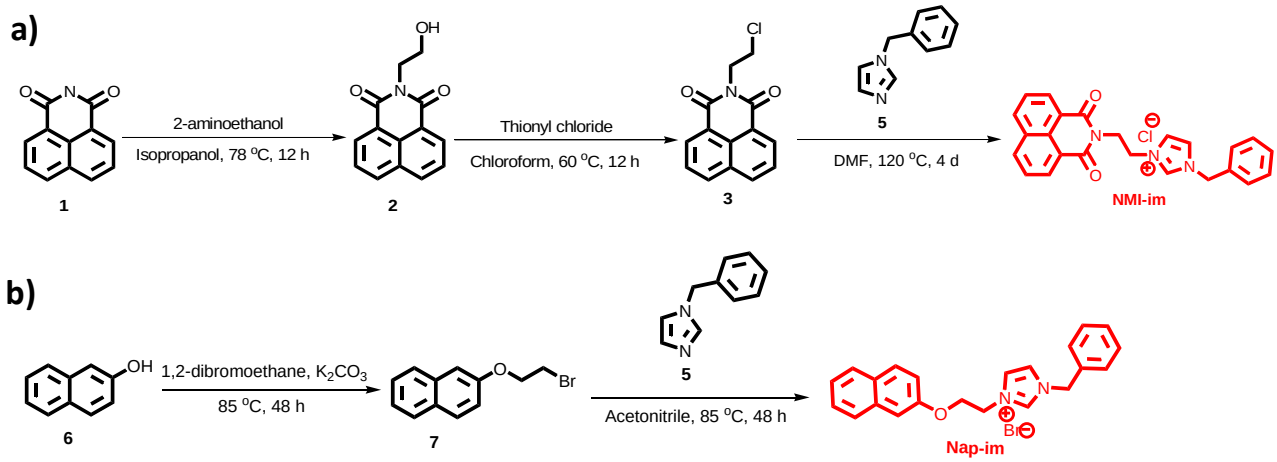

Scheme S2. Synthetic route for synthesising **L1, L2 and L3**.

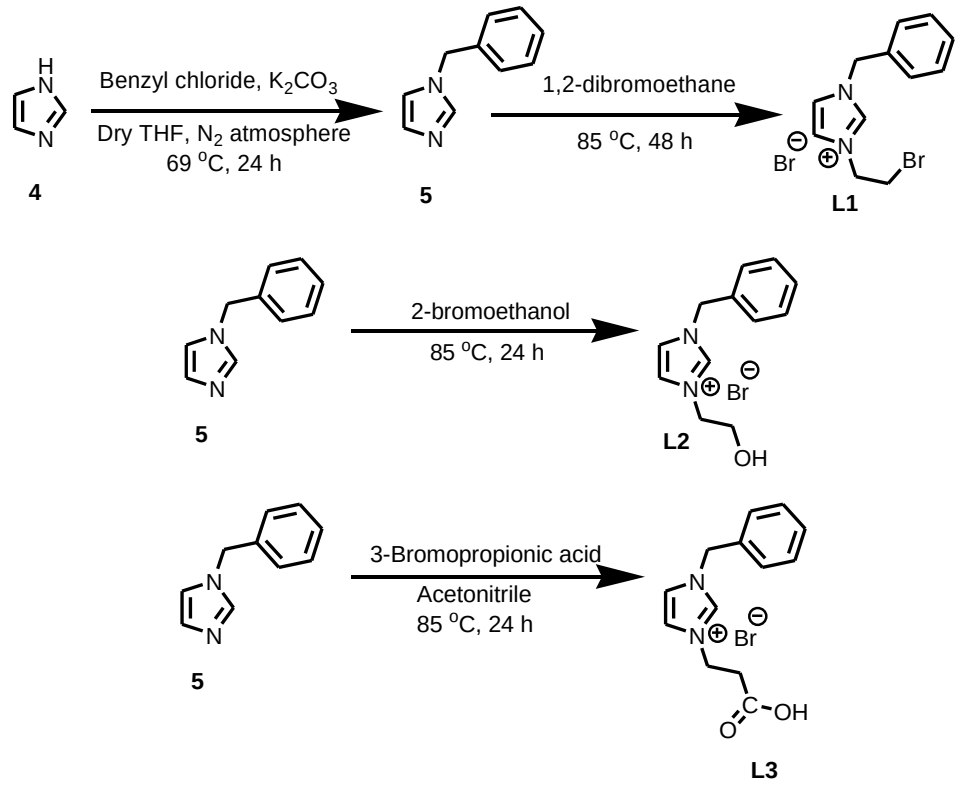

Synthesis of **5**: Molecule **5** was synthesized according to the reported procedure. [S1] 6.8 g of **4,** and 6.9 g of K_2CO_3 was taken in a three necked round bottom flask (RB) and in it 120 mL of dry THF was added and stirred at room temperature for 30 minutes and then benzyl chloride was added dropwise into the solution and the resulting solution was refluxed at 69 ^oC for 24 hours. The progress of the reaction was monitored by TLC and after completion of the reaction excess THF was removed and it was extracted with water and chloroform. The organic layer was then extracted with 1 M HCl. The combined acid layer was then neutralized with $NaHCO_3$ and extracted with DCM. The organic layer was evaporated. The crude was purified using column chromatography with a solvent gradient ranging from chloroform to 5 % methanol in chloroform to obtain the pure product as a white crystalline solid. Yield: 43 %. ^{1}H NMR: (400 MHz, $CDCl_3$, ppm): δ = 7.53 (s, 1H), 7.30-7.36 (m, 3H), 7.13-7.15 (m, 2H), 7.08 (s, 1H), 6.9 (s, 1H), 5.1 (s, 2H); ^{13}C NMR: (100 MHz, $CDCl_3$, ppm): δ = 137.46, 136.28, 129.80, 129.00, 128.26, 127.31, 119.34, 50.78.

Synthesis of **L1**: Molecule **L1** was synthesized according to reported procedure.[S2] 2 g of molecule **5** was taken in a single necked RB and in it 8.73 mL of 1,2-dibromoethane was added and was refluxed at 85 ^oC for two days. After completion of the reaction it was filtered and washed with excess of DCM. The DCM was evaporated and the crude product was purified using column chromatography by eluting with a gradient ranging from chloroform to 10 % methanol in chloroform to obtain a pale yellow viscous oil. Yield: 65 %. ^{1}H NMR: (400 MHz, $CDCl_3$, ppm): δ = 10.72 (s, 1H), 7.75 (s, 1H), 7.42-7.44 (m, 2H), 7.36-7.37 (m, 3H), 7.30 (s, 1H), 5.54 (s, 2H), 4.87 (t, J = 5.6 Hz, 2H), 3.88 (t, J = 5.6 Hz, 2H); ^{13}C NMR: (100 MHz, $CDCl_3$, ppm): δ = 137.56, 133.07, 129.89, 129.83, 129.22, 123.57, 121.93, 53.91, 51.71, 31.16. HRMS (ESI) m/z: calcd for $C_{12}H_{14}BrN_2^+$: 265.0335, found: 265.0310 $[M]^+$; MALDI-TOF (CCA matrix, positive mode): m/z calcd for $C_{12}H_{14}BrN_2^+$: 265.033, found: 264.897 $[M]^+$.

Synthesis of **L2**: 7 g of **5** and 22.11 g of 2-bromoethanol was taken in a single necked RB and refluxed at 85 ^oC for 24 hours. After completion of the reaction excess of 2-bromoethanol was removed in rotary evaporator and the crude product was purified using column chromatography with a solvent gradient ranging from chloroform to 10 % methanol in chloroform to get the pure product as a viscous liquid. Yield: 41 %. ^{1}H NMR: (400 MHz, DMSO-d_6, ppm): δ = 9.38 (s, 1H), 7.87 (t, J = 1.6 Hz, 1H), 7.82 (t, J = 1.6 Hz, 1H), 7.40-7.90 (m, 5H), 5.35 (s, 2H), 4.28 (t, J = 4.8 Hz, 2H), 3.769 (t, J = 4.8 Hz, 2H); ^{13}C NMR: (100 MHz, DMSO-d_6, ppm): δ = 137.33, 135.82, 129.82, 129.56, 129.24, 124.03, 123.09. HRMS (ESI) m/z: calcd for $C_{12}H_{15}N_2O^+$: 203.1179, found: 203.1195 $[M]^+$; MALDI-TOF (CCA matrix, positive mode): m/z calcd for $C_{12}H_{15}N_2O^+$: 203.11, found: 203.49 $[M]^+$.

Synthesis of **L3**: 7 g of **5** and 26.89 g of 3-bromopropionic acid was taken in a two necked RB and in it 50 ml of dry acetonitrile was added and was refluxed at 80 ^oC for 24 hours. After completion of the reaction the acetonitrile was evaporated and the crude was purified using column chromatography with a solvent gradient ranging from chloroform to 20 % methanol in chloroform to get the pure product as viscous liquid. Yield: 14 %. ^{1}H NMR: (400 MHz, DMSO-d_6, ppm): δ = 9.47 (s, 1H), 7.87 (t, J = 1.6, 2H), 7.40-7.46 (m, 5H), 5.49 (s, 2H), 4.41 (t, J =6.8 Hz, 2H), 4.2 (brs, 1H), 2.96 (t, J = 6.4 Hz, 2H); ^{13}C NMR: (100 MHz, DMSO-d_6, ppm): δ = 172.60, 137.62, 135.86, 129.86, 129.64, 129.31, 123.82, 123.27, 52.61, 49.47, 45.88, 34.71.

Synthesis of molecule **2** and **3**: Molecule **2** and **3** were synthesized following literature procedure.[S3]

Synthesis of **NMI-im**: 1 g of **3** and 200 mg of **5** was taken in a two necked RB and in it 20 mL of dry DMF was added and refluxed at 120 ^{o}C for four days. After completion of the reaction excess DMF was evaporated under reduced pressure and the crude product was subjected to a column chromatography with a solvent gradient ranging from chloroform to 5 % methanol in chloroform. The product fraction was dissolved in water and the impurities got crystalized. It was filtered and the water fraction was evaporated to get the pure product. Yield: 20 %. ^{1}H NMR: (400 MHz, DMSO-d_6, ppm): δ = 9.33 (s, 1H), 8.49 (d, J = 8.4 Hz, 2H), 8.44 (d, J = 7.2 Hz, 2H), 7.90-7.92 (m, 2H), 7.71 (s, 1H), 7.42 (s, 1H), 7.34 (t, J = 3.2 Hz, 2H), 7.23 (t, J = 2 Hz, 2H), 5.35 (s, 2H), 4.57 (t, J = 3.6 Hz, 2H), 4.48 (q, J = 2.4, 2H); ^{13}C NMR: (100 MHz, DMSO-d_6, ppm): δ = 163.62, 136.87, 134.76, 134.55, 131.31, 128.96, 128.93, 128.73, 128.26, 127.65, 127.53, 127.18, 123.72, 122.85, 122.51, 121.79, 51.70, 47.90, 30.63. HRMS (ESI) m/z: calcd for $C_{24}H_{20}N_3O_2^+$: 382.1551, found: 382.1552 $[M]^+$; MALDI-TOF (CCA matrix, positive mode): m/z calcd for $C_{24}H_{20}N_3O_2^+$: 382.155, found: 382.126 $[M]^+$.

Synthesis of **7**: 2g of **6** and 2.5 g of K_2CO_3 was taken in a two necked RB and in it 20 mL dry acetonitrile was added and refluxed at 85 ^{o}C for 30 minutes. 10.42 g of 1,2-dibromoethane was then added dropwise to the refluxing solution. After 48 hours the reaction was stopped and filtered and washed with acetonitrile. The acetonitrile layer was evaporated to get the crude product which was further purified by column chromatography using a gradient ranging from hexane to 10 % ethyl acetate in hexane. Yield: 48 %. ^{1}H NMR: (400 MHz, $CDCl_3$, ppm): δ = 7.72-7.86 (m, 3H), 7.43-7.46 (m, 1H), 7.33-7.37 (m, 1H), 7.13-7.19 (m, 2H), 4.42 (t, J = 6.4 Hz, 2H), 3.71 (t, J = 6.4 Hz, 2H); ^{13}C NMR: (100 MHz, $CDCl_3$, ppm): δ = 156.38, 134.74, 130.00, 129.61, 128.02, 127.13, 126.85, 124.29, 119.06, 107.51, 68.21, 29.34. MALDI-TOF (CCA matrix, positive mode): m/z calcd for $C_{12}H_{11}BrO$: 249.999, found: 249.862 $[M]^+$.

Synthesis of **Nap-im**: 3 g of **7** and 1 g of **2** was taken a two necked RB and in it 50 mL dry acetonitrile was added and refluxed at 85 ^{o}C for 2 days. After completion of the reaction acetonitrile was evaporated and the crude was purified by column chromatography using 3 % methanol in chloroform solution. Yield: 80 %. ^{1}H NMR: (400 MHz, $CDCl_3$, ppm): δ = 10.27 (s, 1H), 7.64-7.69 (m, 4H), 7.37 (s, 3H), 7.29-7.31 (m, 4H), 7.22 (s, 1H), 7.10 (s, 1H), 7.03-7.06 (d, 1H), 5.47 (s, 2H), 4.85 (t, J = 6.4 Hz, 2H), 4.43 (t, J = 6.4 Hz, 2H); ^{13}C NMR: (100 MHz, DMSO-d_6, ppm): δ = 155.60, 137.92, 134.58, 132.86, 130.10, 129.97, 129.86, 129.66, 128.28, 127.93, 127.29, 127.07, 124.60, 123.68, 121.58, 118.35, 107.61, 66.59, 53.90, 49.93.. HRMS (ESI) m/z: calcd for $C_{22}H_{21}N_2O^+$: 329.1649, found: 329.1650 $[M]^+$; MALDI-TOF (CCA matrix, positive mode): m/z calcd for $C_{22}H_{21}N_2O^+$: 329.164, found: 329.090 $[M]^+$.

Scheme S3. a) Synthetic route for synthesising exfoliated MoS_2 and **MoS_2-L1**; b) Synthetic route to **FEG** and **Graphene-L2.**

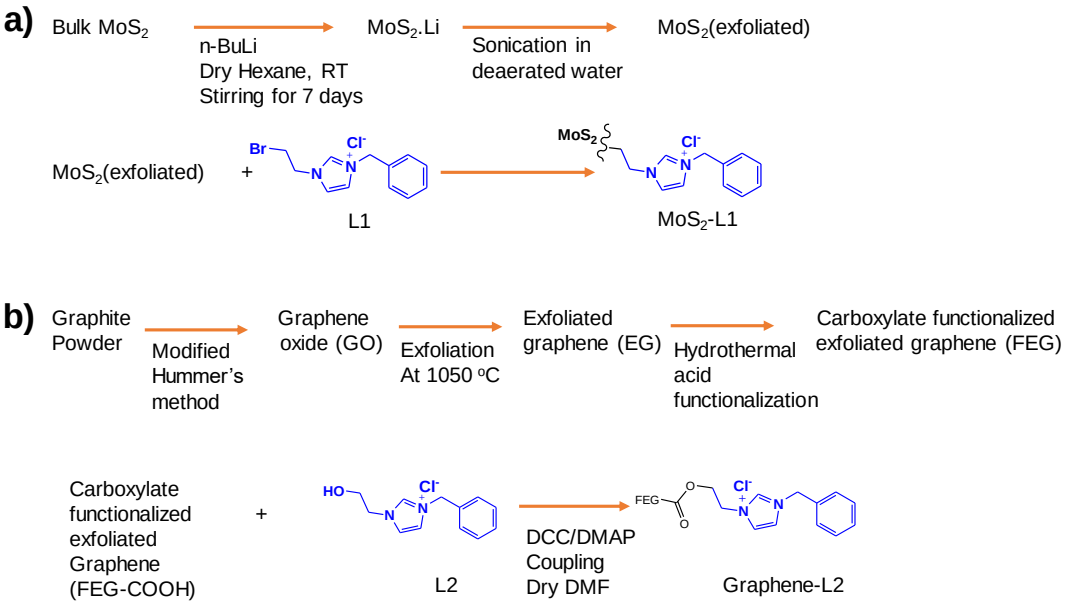

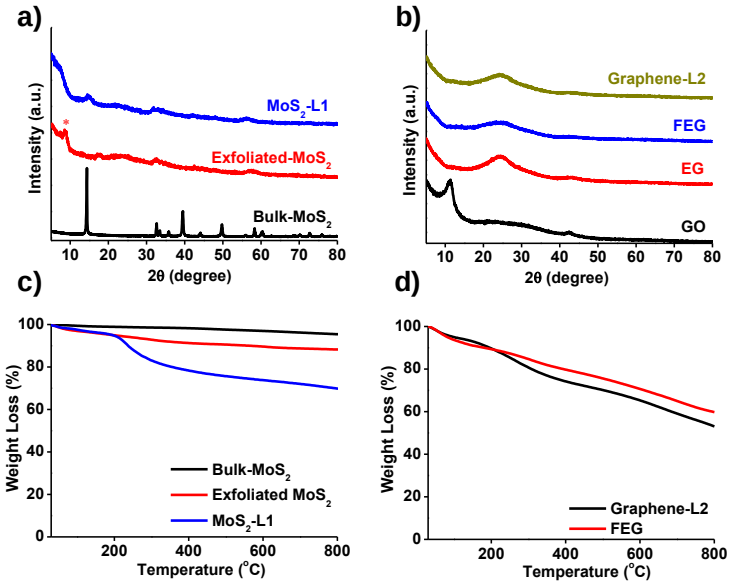

Figure S1. a) PXRD pattern of bulk MoS_2, exfoliated MoS_2, **L1** functionalized MoS_2; b) PXRD pattern of graphene oxide (**GO**), exfoliated graphene (**EG**), carboxylate functionalized exfoliated graphene (**FEG**) and **Graphene-L2**; c) Thermogravimetric analysis of **MoS_2-L1** in comparison to exfoliated and bulk MoS_2 showing weight loss of 15 wt%; d) for **Graphene-L2** in comparison to carboxylate functionalized graphene (**FEG**) showing weight loss of 6 wt%.

Note: The red asterisk marked peak at $2\theta = 8.9°$ indicates the increase in interlayer spacing due to exfoliation in comparison to bulk MoS_2.

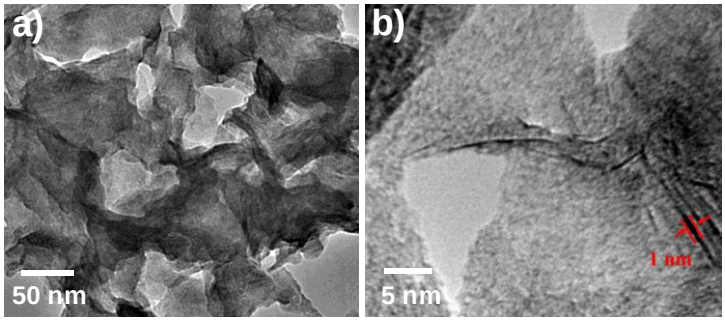

Figure S2. a) TEM image showing the **MoS_2-L1** nanosheet; b) corresponding HRTEM image showing the presence of **MoS_2-L1** layers with an interlayer spacing of 1 nm.

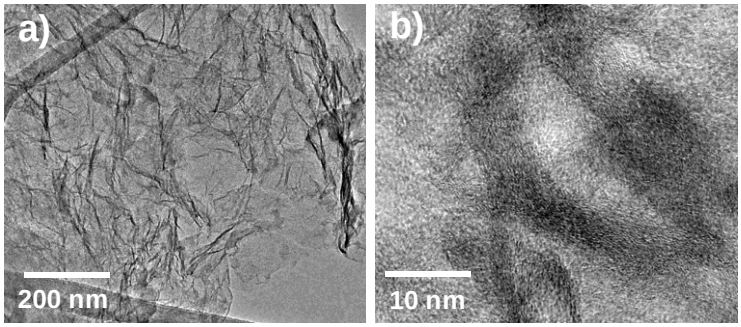

Figure S3. a) TEM image showing the **Graphene-L2** nanosheet; b) corresponding HRTEM image showing the presence of **Graphene-L2** layers.

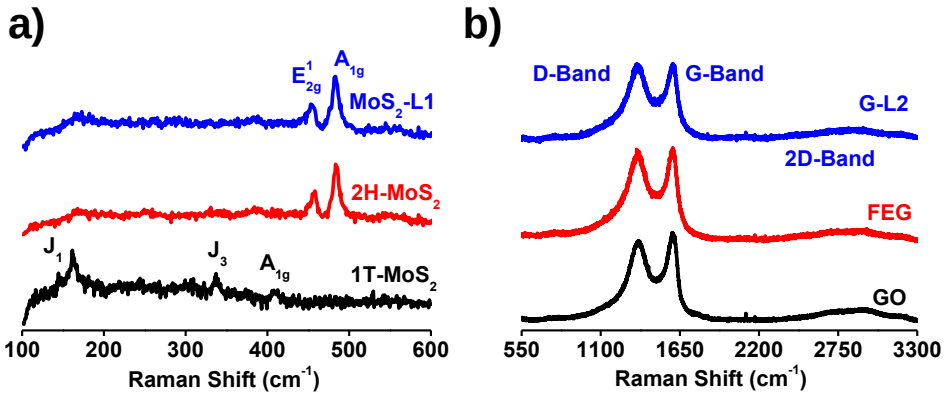

Figure S4. a) Raman spectra of chemically exfoliated 1T-MoS_2, 2H-MoS_2 (obtained from settling of 1T-MoS_2) and **MoS_2-L1**; b) Raman spectra of graphene oxide (**GO**), carboxylate functionalised graphene (**FEG**) and **L2** functionalised **FEG** i.e. **Graphene-L2**.

Note: Raman analysis (Figure S4a) shows the presence of J_1 and J_3 at 197 and 336 cm^{-1} which are the characteristic for 1T-MoS_2. Whereas, on settling of 1T-MoS_2, 2H-MoS_2 is formed which gives peaks at 383 and 406 cm^{-1} corresponding to E^1_{2g} (out of plane vibration mode) and A_{1g} (in plane vibration mode) modes, respectively. The similar vibration modes have been observed for **MoS_2-L1.** D and G band in case of **GO, FEG** and **Graphene-L2** has been observed at 1357 and 1614 cm^{-1} which correspond to disorders in graphene structures and C-C vibrational mode of sp^2 hybridised carbons, respectively (Figure S4b). 2D band is observed at 2845 cm^{-1}.

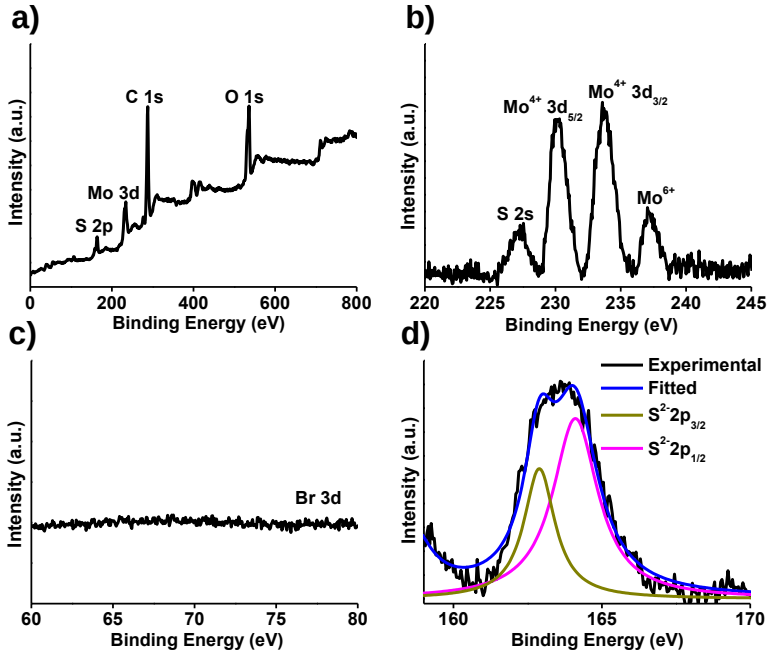

Figure S5 a) X-ray photoelectron spectrum of **L1** functionalised MoS_2 ; b) High resolution XPS of **MoS_2-L1** showing the peaks for Mo^{4+} $3d_{3/2}$ and Mo^{4+} $3d_{5/2}$; c) High resolution XPS of **MoS_2-L1** showing the absence of Br signal in **MoS_2-L1**; d) High resolution XPS of **MoS_2-L1** showing the peaks for S^{2-} $2p_{3/2}$ and S^{2-} $2p_{1/2}$.

Table S1: Comparison of binding energies for bulk MoS_2 and MoS_2-L1

	Binding energy (eV)			
Compound	Mo^{4+} $3d_{5/2}$	Mo^{4+} $3d_{3/2}$	S^{2-} $2p_{3/2}$	S^{2-} $2p_{1/2}$
Bulk MoS_2	229.4	232.6	163.2	163.5
MoS_2-L1	230.1	233.7	162.8	164.1

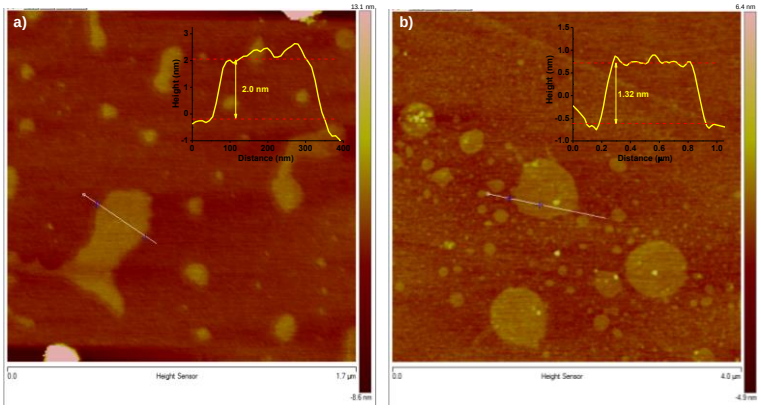

Figure S6 a) Atomic force microscopy images for a) **MoS_2-L1** b) **Graphene-L2** with inset graphs showing the height profiles for **MoS_2-L1 (2.0 nm)** and **Graphene-L2 (1.32 nm)**.

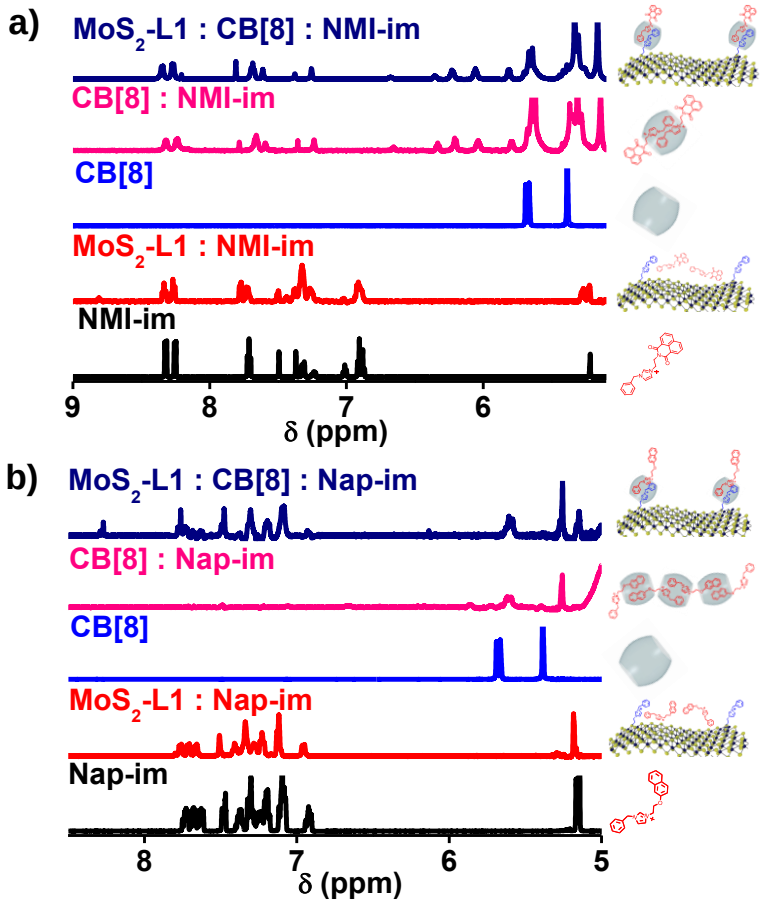

Figure S7. a) ^{1}H-NMR spectra showing the non-covalent functionalization of **MoS_2-L1** with **NMI-im** in presence of CB[8] using efficient ternary complexation between imidazole groups. Selective Shift in benzene and imidazole peaks of **MoS_2-L1 :** CB[8] **: NMI-im** non-covalent hybrid confirms the ternary complex formation (navy blue curve). Corresponding blank of **MoS_2-L1** and **NMI-im** in absence of CB[8] does not show any shift of protons confirming absence of any ground state interaction between MoS_2 and **NMI-im** (red curve). ^{1}H-NMR of CB[8] and CB[8] : **NMI-im** are shown for comparison, where CB[8] : **NMI-im** forms ternary complex between benzyl imidazole groups of **NMI-im** as can be seen from selective shift of benzene and imidazole protons (pink curve). Corresponding schematics explaining the respective ^{1}H-NMR are shown in side;

b) ^{1}H-NMR spectra of **MoS_2-L1**, **Nap-im** in presence of CB[8] shows similar observation as above confirming the ternary complex formation and functionalization of MoS_2 with naphthol (navy blue curve). Corresponding blank of **MoS_2-L1** and **Nap-im** in absence of CB[8] does not show any shift in the protons confirming absence of any ground state interaction between MoS_2 and donor (pink curve). ^{1}H-NMR of CB[8] and CB[8] : **NMI-im** are shown for comparison where unlike **NMI-im**, in addition to the formation of ternary complex between benzyl imidazole groups of **Nap-im**, the napthol protons also form ternary complex in CB[8] host due to which all the protons of **Nap-im** are shifted depicting interaction between naphthol chromophore and CB[8] (**NMI-im** = **Nap-im** =10^{-4} M, CB[8] = 10^{-4} M, H_2O). Corresponding schematics explaining the respective ^{1}H-NMR are shown in side.

Note: The ^{1}H-NMR of CB[8] : **NMI-im** shows similar shift of benzene protons only as that have been observed for **MoS_2-L1 :** CB[8] **: NMI-im** due to ternary complex formation between two **NMI-im** inside CB[8] cavity.

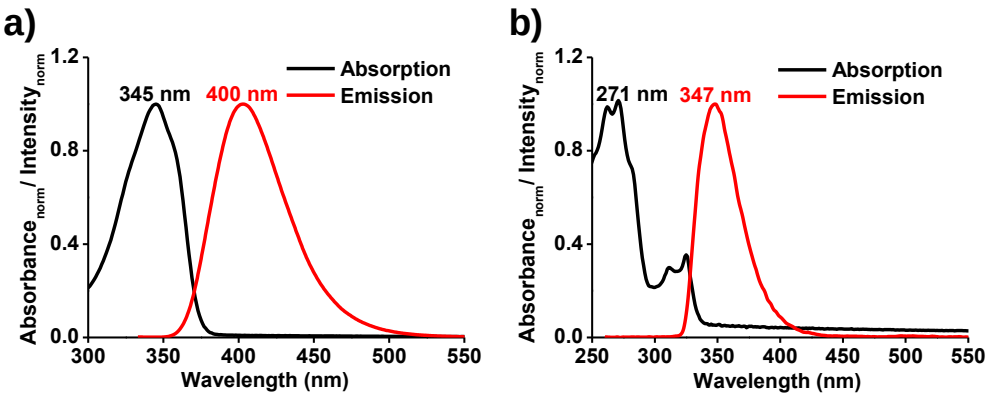

Figure S8. Absorption and emission spectra of a) **NMI-im**; b) **Nap-im** in water (**NMI-im** = **Nap-im** =10^{-4} M, CB[8] = 10^{-4} M, H_2O)

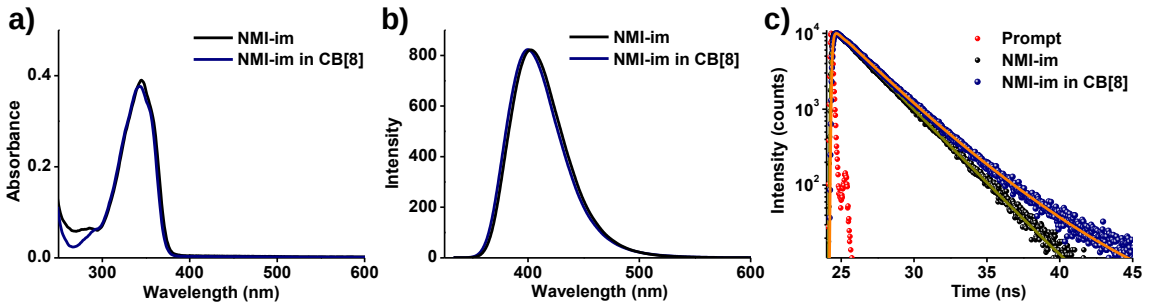

Figure S9. a) Absorption spectra; b) emission spectra (λ_{ex} = 323 nm) for **NMI-im** in presence and absence of CB[8] in water showing no change in absorption or emission spectra of the chromophore; c) Corresponding lifetime decay profile (λ_{ex} = 373 nm, λ_{coll} = 400 nm) for **NMI-im** in the presence and absence of CB[8] in water with negligible difference between them (**NMI-im** = 10^{-4} M, CB[8] = 10^{-4} M, H_2O).

Note: Unchanged spectral properties of **NMI-im** in presence of CB[8] suggests that NMI chromophore does not go inside CB[8] cavity to form any kind of ternary complex. Only the benzyl imidazole group forms a ternary complex with CB[8] thus corroborating with the earlier observation with ^{1}H-NMR.

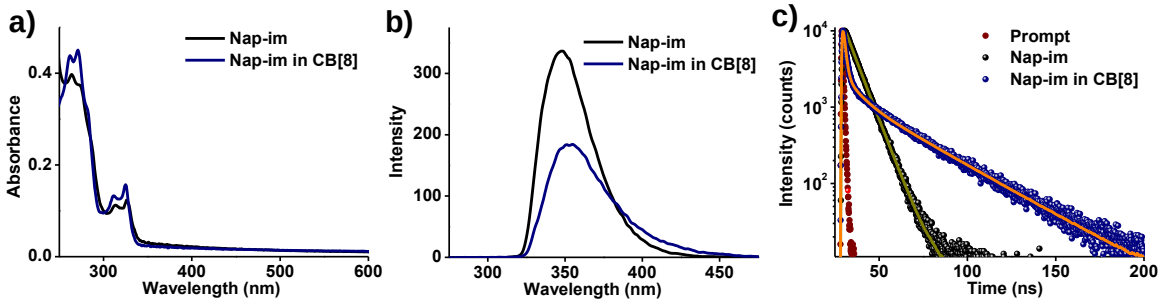

Figure S10. a) Absorption spectra; b) emission spectra (λ_{ex} = 250 nm) for **Nap-im** in water showing shift in absorption and emission spectra in the presence of CB[8] than that of **Nap-im** in water without CB[8]; c) Corresponding lifetime decay profile (λ_{ex} = 286 nm, λ_{coll} = 350 nm) for **Nap-im** in water in the presence and absence of CB[8] with considerable difference between them (**Nap-im** = 10^{-4} M, CB[8] = 10^{-4} M, H_2O).

Note: Shift in absorption and emission spectra of **Nap-im** in presence of CB[8] in water suggests that naphthol chromophores are going inside CB[8] cavity to form a ternary complex which leads to formation of a supramolecular polymers. Since both naphthol and imidazole group is forming a ternary complex in this case, we observe shift in all the protons of **Nap-im** in presence of CB[8] as observed by ^{1}H-NMR experiment. Further confirmation of interaction between two naphthol chromophore inside CB[8] cavity comes from the lifetime decay experiment, where presence of a sharp decay component depicts π-π interaction and quenching of fluorescence is observed.

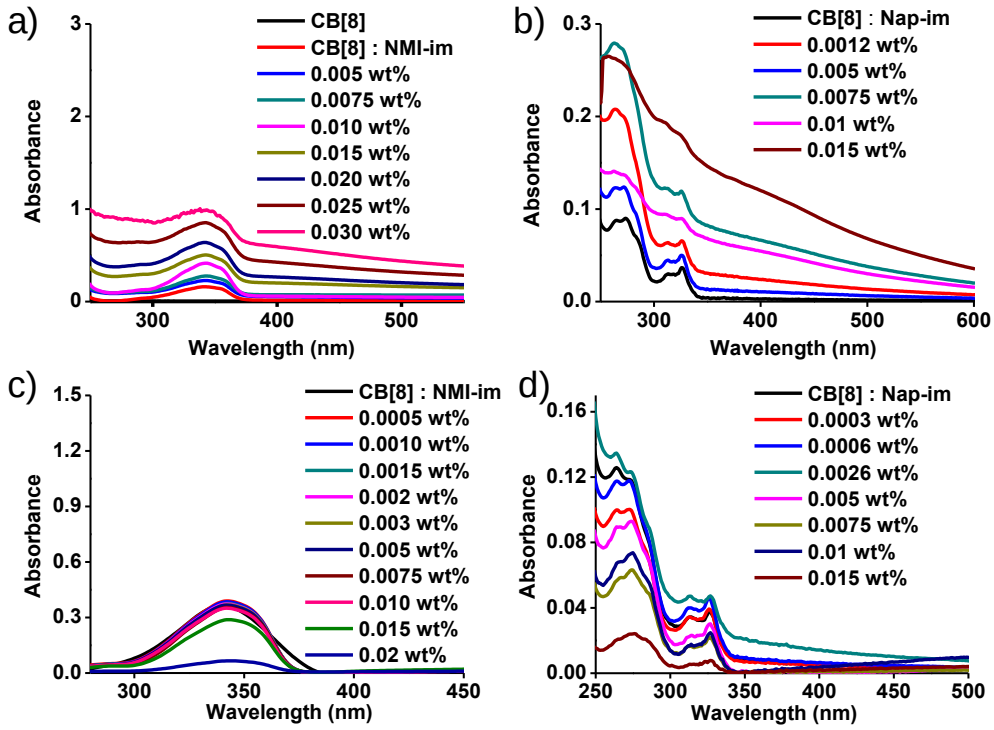

Figure S11. Absorption spectra of NMI-**im** with increasing amount of a) **MoS_2-L1**; c) **Graphene-L2** and absorption spectra of **Nap-im** with increasing amount of b) **MoS_2-L1**; d) **Graphene-L2** in presence of CB[8] (**NMI-im** = **Nap-im =** 10^{-4} M, CB[8] = 10^{-4} M, H_2O)**.**

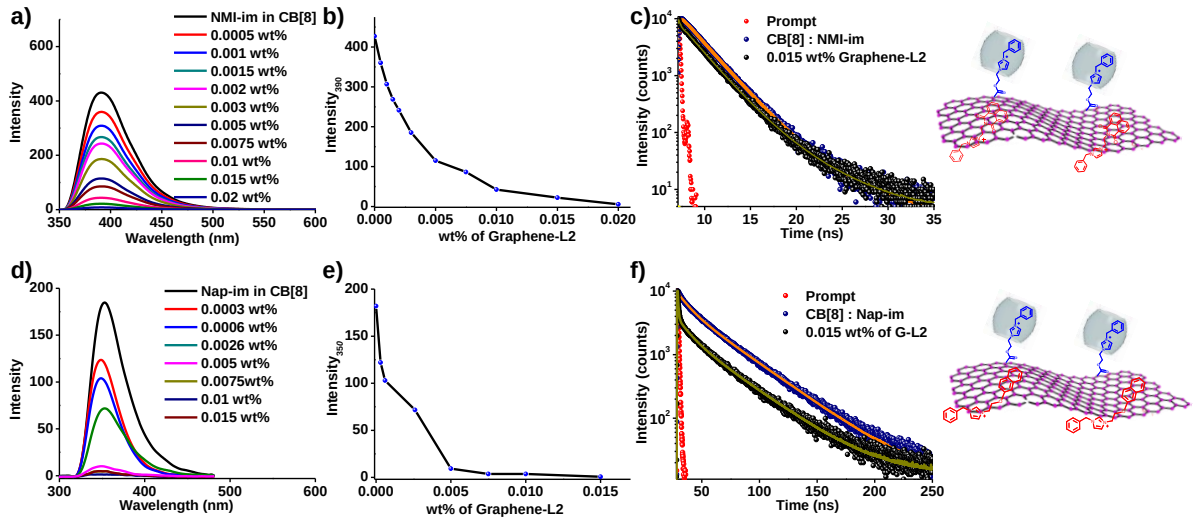

Figure S12. a) Fluorescence spectra of **NMI-im** in presence of CB[8] and increasing wt% of **Graphene-L2** showing gradual quenching of fluorescence; b) corresponding titration plot showing complete quenching with 0.015 wt% of **Graphene-L2**; c) Respective lifetime decay profile of **NMI-im** in CB[8] and **NMI-im** in presence of **Graphene-L2** and CB[8] with almost no change in life-time with or without **Graphene-L2** suggesting that it is due to the residual monomers and hence the fluorescence quenching would be due to ground state π-π or charge-transfer interaction between **NMI-im** and **Graphene-L2**; inset shows the corresponding schematic of π-π interaction between **NMI-im** and **Graphene-L2**; d) Fluorescence spectrum of **Nap-im** in presence of CB[8] and increasing wt% of **Graphene-L2** showing gradual quenching of fluorescence; e) corresponding titration plot showing saturation of fluorescence quenching with 0.015 wt% of **Graphene-L2**; f) Corresponding lifetime decay profile of **Nap-im** in CB[8] and **Nap-im** in presence of **Graphene-L2** and CB[8] showing decrease in lifetime indicating towards ground state interaction through π-π or charge-transfer interaction along with excited state interaction; in inset corresponding schematic showing the π-π interaction between **Nap-im** and **Graphene-L2**. (**NMI-im** = **Nap-im** = 10^{-4} M, CB[8] = 10^{-4} M, H_2O).

Note: Unchanged lifetime decay profile of **NMI-im** in non-covalent composite and that of only **NMI-im** suggests that the emission is due to residual monomer, thus indicating exclusive ground state interaction through π-π or charge-transfer interaction. Whereas, in the case of **Nap-im** change in lifetime decay profile of **Nap-im** in non-covalent composite and that of only **Nap-im** suggests napthol case would be combination of ground state and excited state interactions (quenching in life time).

Non-covalent Functionalization of BN using Host-Guest Chemistry

In order to test the versatility of the host-guest strategy to various 2-D materials the non-covalent functionalization of BN nanosheets with **NMI-im** have also been attempted which behaved similar to graphene. Synthesis (Scheme S4a) for BN nanosheets, covalent functionalization with **L3** (Scheme S4b) and their characterization (Figure S13) has been shown here. The non-covalent functionalization of **BN-L3** was performed with **NMI-im** and spectroscopic studies were performed. Figure S14a shows the absorption spectra of **NMI-im** with increasing wt% of **BN-L3**. Broadening in the absorption spectra with increasing wt% of **BN-L3** may be attributed to the presence of ground state interactions among the **BN-L3** and NMI chromophore. Quenching of fluorescence is observed with increasing wt% of **BN-L3** (Figure S14b) and, complete quenching is observed at 0.05 wt% of **BN-L3** (Figure S14c)**.** Life time decay studies (Figure S14d) shows significant quenching of NMI lifetime along with appearance of very fast components (Table S6). Since complete ground state interaction would have quenched the fluorescence and lifetime would have come from residual monomers, in this case appearance of a completely different lifetime spectra suggests presence of both ground state as well as excited state interaction. ^{1}H NMR studies (Figure S15) indicates the absence of any ground state interactions between **BN-L3** and **NMI-im** in the absence of CB[8]**.** The phenyl (6.90-7.03 ppm) and imidazole (7.2-7.5 ppm) ring protons of the **NMI-im** exhibit upfield shifts to 5.30 and 5.60 ppm, respectively in presence of the CB[8] at 0.015 wt % of **BN-L3** indicating the formation of host-guest ternary complex between the benzyl imidazole groups of **BN-L3** and **NMI-im** (Figure S15)**.** Whereas, at higher concentrations of **BN-L3** (0.05 wt%) complete shifting of the proton signals is observed.

Scheme S4. Synthesis of a) BN nanosheets; b) **BN-L3** by EDC coupling reaction

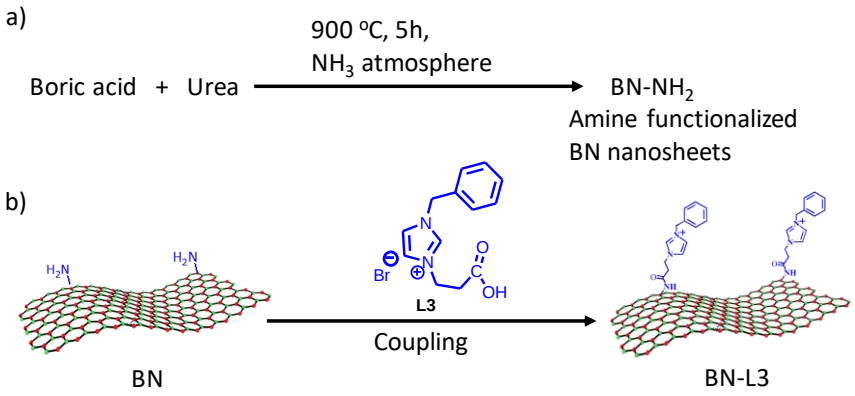

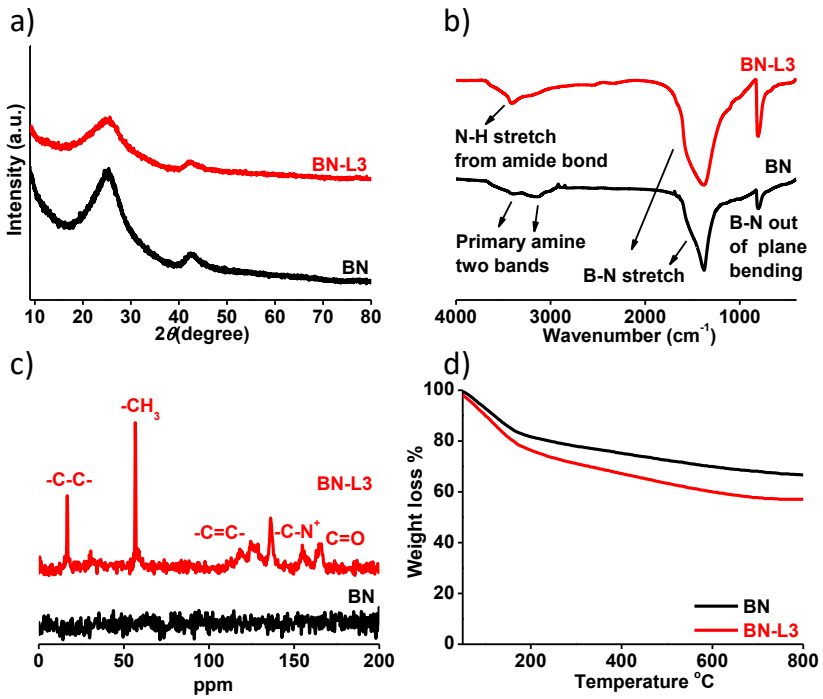

Figure S13. a) Powder X-ray diffraction pattern for **BN** and **BN-L3**; b) Infra-red spectra for BN and **BN-L3**; c) ^{13}C solid state NMR for BN and **BN-L3;** d) Thermogravimetric analysis for BN and **BN-L3.**

Note: Powder X-ray pattern for BN and **BN-L3** shows 2θ peaks at 25.1° and 42.1° indicating the formation of BN. IR spectra for BN shows characteristic peaks at 1379 cm^{-1} and 798 cm^{-1} for B-N stretching and B-N out of plane bending respectively. IR spectra of BN shows the stretching frequencies at 3391 cm^{-1} and 3125 cm^{-1} corresponding to the primary amine stretching whereas in the spectra for **BN-L3** stretching corresponding to that of N-H stretch from amide bond is observed. ^{13}C solid state NMR of BN does not show any signal whereas that of **BN-L3** shows signal at 16 and 56 ppm indicating the presence of aliphatic carbons of **L3**. Signals corresponding to the 100-150, 155 and 165 ppm are observed signifying the presence of aromatic carbons, -C-N^+, C=O (from amide bond formation) respectively from **L3.** Thermogravimetric analysis shows weight loss of 10 wt% in case of BN in comparison to **BN-L3**.

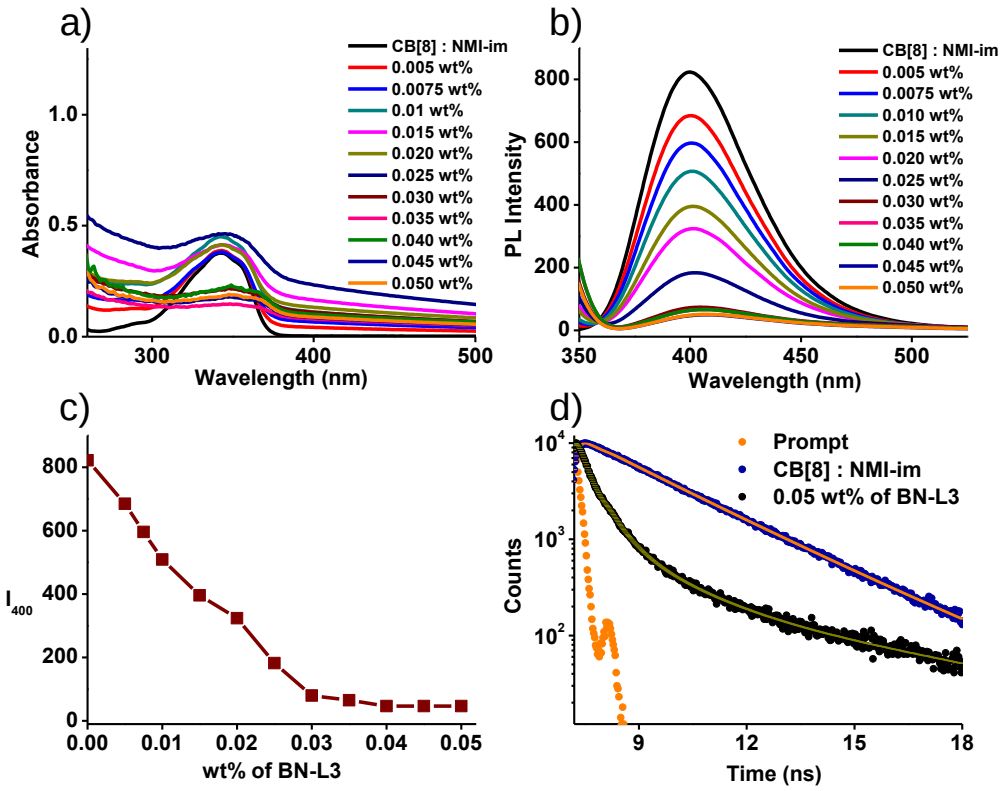

Figure S14. a) Absorption spectra of **NMI-im** with increasing amount of **BN-L3**; b) Fluorescence spectra of **NMI-im** in presence of CB[8] and increasing wt% of **BN-L3** showing gradual quenching of fluorescence; c) corresponding titration plot showing complete quenching with 0.05 wt% of **BN-L3**; c) Respective lifetime decay profile of **NMI-im** in CB[8] and **NMI-im** in presence of **BN-L3** and CB[8] (**NMI-im** = 10^{-4} M, CB[8] = 10^{-4} M, H_2O).

Note: Gradual broadening of absorbance spectra with increasing amount of **BN-L3** suggests presence of ground state charge transfer interaction between BN and NMI chromophore. Decrease in lifetime suggests presence of both non-covalent functionalization and ground state interaction in case of NMI chromophore.

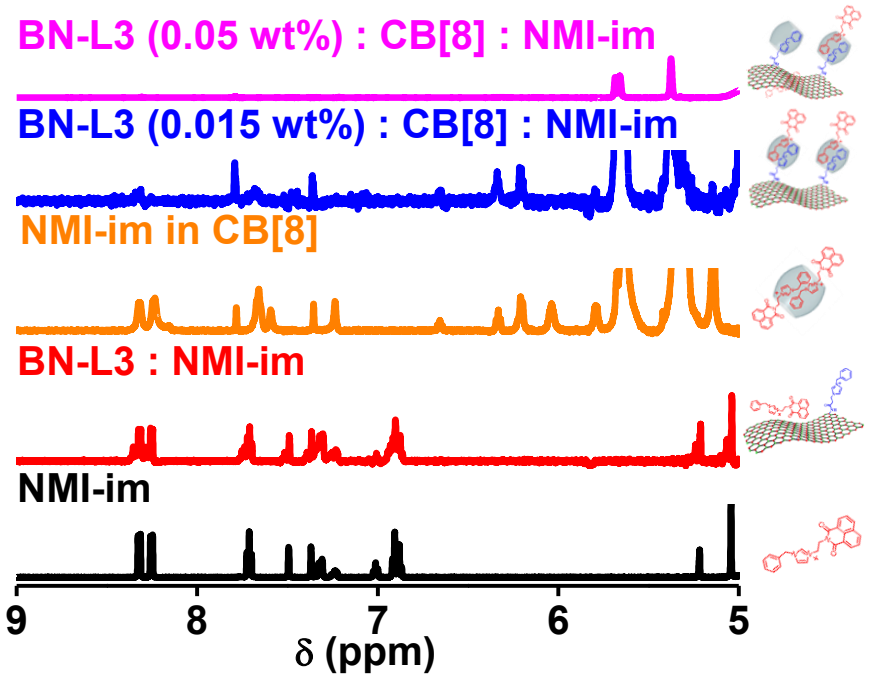

Figure S15. ^{1}H-NMR spectra showing the non-covalent functionalization of **BN-L3** with **NMI-im** in presence of CB[8] using efficient ternary complexation between benzyl imidazole groups. Selective Shift in benzene and imidazole peaks of **BN-L3 (0.015 wt%) :** CB[8] **: NMI-im** non-covalent hybrid confirms the ternary complex formation (blue curve). Corresponding blank of **BN-L3** and **NMI-im** in absence of CB[8] does not show any shift of protons confirming absence of any ground state interaction between **BN-L3** and **NMI-im** (red curve). ^{1}H-NMR of CB[8] : **NMI-im** are shown for comparison, where CB[8] : **NMI-im** forms ternary complex between benzyl imidazole groups of **NMI-im** as can be seen from selective shift of benzene and imidazole protons (orange curve). Increasing the wt% of **BN-L3 upto 0.05 wt% (pink curve)** has shown the complete shift of protons indicating the agglomeration of **NMI-im** at higher concentrations of **BN-L3;** Corresponding schematics explaining the respective ^{1}H-NMR are shown in side; (**NMI-im** = 10^{-4} M, CB[8] = 10^{-4} M, H_2O).

Table S2: Lifetime data for **NMI-im** : CB[8] and **MoS_2-L1** : CB[8] : **NMI-im** non-covalent hybrid (λ_{ex} = 373 nm, λ_{coll} = 400 nm)

Compound	T_1 (ns) (Rel. amp)	T_2(ns) (Rel. amp)	T_3(ns) (Rel. amp)
NMI-im : CB[8]	2.18 (78.60)	3.42 (21.40)	
MoS_2-L1 : CB[8] : **NMI-im**	2.26 (73.39)	6.62 (9.99)	0.02 (16.63)

Table S3: Lifetime decay studies for **Nap-im** : CB[8] and **MoS_2-L1** : CB[8] : **Nap-im** non-covalent hybrid (λ_{ex} = 286 nm, λ_{coll} = 350 nm)

Compound	T_1 (ns) (Rel. amp)	T_2(ns) (Rel. amp)	T_3(ns) (Rel. amp)	T_4(ns) (Rel. amp)
Nap-im : CB[8]	2.47 (3.02)	7.25 (96.98)		
MoS_2-L1 : CB[8] : **Nap-im**	6.97 (13.30)	23.4 (13.31)	59.7 (3.03)	0.03 (70.36)

Table S4: Lifetime decay studies for **NMI-im** : CB[8] and **Graphene-L2** : CB[8] : **NMI-im** non-covalent hybrid (λ_{ex} = 373 nm, λ_{coll} = 400 nm)

Compound	T_1 (ns) (Rel. amp)	T_2(ns) (Rel. amp)	T_3(ns) (Rel. amp)
NMI-im : CB[8]	2.18 (78.60)	3.42 (21.40)	
Graphene-L2 : CB[8] : **NMI-im**	2.22 (87.61)	4.36 (9.35)	0.03 (3.04)

Table S5: Lifetime decay studies for **Nap-im** : CB[8] and **Graphene-L2** : CB[8] : **Nap-im** non-covalent hybrid (λ_{ex} = 286 nm, λ_{coll} = 350 nm)

Compound	T_1 (ns) (Rel. amp)	T_2(ns) (Rel. amp)	T_3(ns) (Rel. amp)
Nap-im : CB[8]	9.78 (13.93)	33.8 (81.02)	0.09 (5.05)
Graphene-L2 : CB[8] : **Nap-im**	10.0 (10.41)	33.4 (49.74)	0.036 (39.85)

Table S6: Lifetime decay studies for **NMI-im** : CB[8] and **BN-L3**: CB[8] : **NMI-im** non-covalent hybrid (λ_{ex} = 373 nm, λ_{coll} = 400 nm)

Compound	T_1 (ns) (Rel. amp)	T_2(ns) (Rel. amp)	T_3(ns) (Rel. amp)	T_4(ns) (Rel. amp)
NMI-im : CB[8]	1.82 (24.98)	2.55 (71.80)	4.46 (3.22)	
BN-L3: CB[8] : **NMI-im**	0.46 (40.39)	1.47 (22.10)	5.90 (18.95)	0.12 (18.57)

References

[S1] Zhou, Y.; Gong, Y. Asymmetric Copper(II)-Catalysed Nitroaldol (Henry) Reactions Utilizing a Chiral C_1-Symmetric Dinitrogen Ligand. *Eur. J. Org. Chem.* **2011**, *30*, 6092–6099.

[S2] Yuan, D.; Tang, H.; Xiao, L.; Huynh, H. V. CSC-Pincer versus Pseudo-pincer Complexes of palladium(II): A Comparative Study on Complexation and Catalytic Activities of NHC complexes. *Dalton Trans*. **2011**, *40*, 8788–8795.

[S3] Shelton, A. H.; Shazanovich, I. V.; Weinstein, J. A.; Ward, M. D. Controllable Three-component Luminescence from a 1,8-Naphthalimide/Eu(III) complex: White Light Emission from a Single Molecule. *Chem. Commun*. **2012**, *48*, 2749-2751.